Sodium abundances in nearby disk stars ⋆

J.R. Shi[1,2], T. Gehren[2], and G. Zhao[1,2]

[1] National Astronomical Observatories, Chinese Academy of Sciences, Beijing 100012, P. R. China
[2] Institut für Astronomie und Astrophysik der Universität München, Scheinerstrasse 1, D-81679 München, Germany

Abstract. We present sodium abundances for a sample of nearby stars. All results have been derived from NLTE statistical equilibrium calculations. The influence of collisional interactions with electrons and hydrogen atoms is evaluated by comparison of the solar spectrum with very precise fits to the Na I line cores. The NLTE effects are more pronounced in metal-poor stars since the statistical equilibrium is dominated by collisions of which at least the electronic component is substantially reduced. The resulting influence on the determination of sodium abundances is in a direction opposite to that found previously for Mg and Al. The NLTE corrections are about -0.1 in thick-disk stars with [Fe/H] ~ -0.6. Our [Na/Fe] abundance ratios are about solar for thick- and thin-disk stars. The increase in [Na/Fe] as a function of [Fe/H] for metal-rich stars found by Edvardsson et al. (1993) is confirmed. Our results suggest that sodium yields increase with the metallicity, and quite large amounts of sodium may be produced by AGB stars. We find that [Na/Fe] ratios, together with either [Mg/Fe] ratio, kinematic data or stellar evolutionary ages, make possible the individual discrimination between thin- and thick-disk membership.

Key words. Line: formation-Line:profiles-Stars: abundances-Stars:cool- Galaxy:evolution

1. Introduction

The ^{23}Na nucleus contains an extra neutron that makes its synthesis deviate from that of the α-nuclei such as ^{24}Mg. So the abundance ratios [Na/Fe] and/or [Na/Mg] in stars are a potential source of information concerning the history of Galactic nucleosynthesis.

It is expected that sodium is made during carbon and neon burning in massive stars, and it would therefore be ejected by Type II supernova (SN II). Type Ia supernova, on the other hand, produce little sodium (Tsujimoto et al. 1995). However, ^{23}Na can be synthesized as a primary or secondary element. In the first case ^{23}Na would be produced directly in the carbon burning process, and the production rate would be independent of the metal content of the proceeding stellar generation. In the second process, where ^{23}Na is produced by an excess of neutrons, the production rate would depend on that neutron excess which in turn would be determined by the pre-existing metal-abundance. In the latter case ^{23}Na would be expected to display an underabundance compared with Fe or Mg in the most metal-poor stars. Although significant progress has been made in nucleosynthesis calculations, theoretical SN yields of sodium have not yet converged to consistency among models from different authors (Woosley & Weaver 1995; Limongi et al. 1998; Umeda et al. 2000). Also some synthesis of sodium in intermediate-mass stars can occur in the hydrogen-

burning shell through the neon-sodium cycle (Denissenkov & Denissenkova 1990; Mowlavi 1999).

The observational picture for this element is complicated. The early studies report that sodium scales with iron at all metallicities (e.g. the review of Timmes et al. 1995 and Goswami & Prantzos 2000). However, new studies do not support this classical picture. For metal-poor stars, Pilachowski et al. (1996) analyzed a sample of 60 halo subgiants, giants and horizontal branch stars in the interval $-3 \leq$ [Fe/H] ≤ -1, and found a small [Na/Fe] deficiency of -0.17 dex in the mean and that bright field halo giants do not show the excess of sodium found in their globular cluster counterparts. Baumüller et al. (1998) performed a NLTE analysis of sodium and reported a clear trend of decreasing [Na/Fe] with decreasing metallicity. Similarly, Stephens (1999) found that [Na/Fe] decreases as one goes from [Fe/H]$= -1$ to [Fe/H]$= -2$, and thus shows the theoretically expected behaviour of odd-Z elements. Carretta et al. (2000) and Gratton et al. (2003) also found that sodium is overdeficient in stars with [Fe/H] ≤ -1; this result was confirmed by very recent work of Gehren et al. (2004).

For disk stars, Edvardsson et al. (1993) used high-resolution, low-noise spectra to determine sodium abundace in 189 F and G stars. Their LTE analysis suggested that the [Na/Fe] ratio is solar and varies very little with metallicity, which was confirmed by Chen et al. (2000). Based on 5682/5688 and 6154/6160 lines, Prochaska et al. (2000) measured sodium **abundance** in their thick-disk stars and found that all the stars show mildly enhanced [Na/Fe] and there is a mild trend with metallicity (see also Gehren et al. 2004).

Concerning the most metal-rich stars in the galactic disk, the study by Edvardsson et al. (1993) raised a number of new questions. They found sodium relative iron versus [Fe/H] **shows** an increase for [Fe/H] > 0.0 (see also Feltzing & Gustafsson 1998, their Fig. 8). Is the "upturn" real? Large star-to-star scatter was encountered. Could this scatter to be reduced by using better abundance criteria?

It is known that [Fe/H] distributions of the halo, thick- and thin-disk stars reveal considerable overlap, so it can not allow for an unequivocal classification for many stars without reference to other criteria such as age or kinematics. Fuhrmann (1998, 2002) suggested that the thick-disk stars represent the principal population for the early Galactic evolution, while the stellar halo contributes by only minute amounts (see also Ryan & Smith 2003). Considering the general kinematics, there may be a significant overlap of all populations (Gehren et al. 2004). Gratton et al. (1996, 2000, 2003) have shown that thick-disk stars are more [Mg/Fe] enhanced than the thin-disk stars at the same [Fe/H] value. This trend has also been reported by Fuhrmann (1998; see also Prochaska et al. 2000 and Reddy et al. 2003). Finally, Mashonkina et al. (2003) have given evidence that [Eu/Mg] ratio allows the individual discrimination of halo stars from thick-disk stars, and a similar behaviour is found for the [Al/Mg] ratio by Gehren et al. (2004).

The present work is based on a sample of nearby stars and aims at exploring their [Na/Fe] abundance ratios applying full spectrum synthesis based on level populations calculated from the statistical equilibrium equations. In Sect. 2 we present the observational techniques, while the atmospheric models and stellar parameters are discussed in Sect. 3. NLTE line formation is discussed in Sect. 4. The discussion is presented in Sect. 5, and the conclusions are found in the last section.

2. Observations

Our approach towards a representative abundance investigation is aimed at analyzing a volume-complete sample of the F, G and early K dwarfs in the disk population, north of a declination of $\delta = -15°$ and within 25pc of the Sun (see Fuhrmann 2004, for details). The spectra of our samples were obtained through the years 1995 to 2000 by Klaus Fuhrmann with the fiber-coupled Cassegrain échelle spectrograph FOCES (Pfeiffer et al. 1998) mounted at the 2.2m telescope of the Calar Alto Observatory. Only few of them were exposed to a 1024^2 24μ CCD with $\lambda/\Delta\lambda \sim 40000$, and their wavelength ranges are limited to 4000-7000 Å, whereas the standard configuration was a 2048^2 15μ CCD that covered 4000-9000 Å with $\lambda/\Delta\lambda \sim 60000$. All stars were observed at least twice with a signal-to-noise ratio of at least S/N ~ 150 up to S/N ~ 400 (see Fuhrmann 1998, 2000, for details).

3. Atmospheric models and stellar parameters

3.1. Model atmospheres

Our analyses are all based on the same type of atmospheric model, irrespective of temperature, gravity or metal abundance. We use line-blanketed LTE model atmospheres, generated as

discussed by Fuhrmann et al. (1997). The main characteristics are:

- the iron opacity was calculated with the improved meteoritic value $\log \varepsilon_{\mathrm{Fe}} = 7.51$
- opacities for metal-poor stars with [Fe/H] < -0.6 were calculated using α-element (O, Ne, Mg, Si, S, Ar, Ca and Ti) abundances enhanced by 0.4 dex
- the mixing-length parameter l/H_p was adopted to be 0.5 (see Fuhrmann et al. 1993)

3.2. Stellar parameters

For most of the stars we adopt the stellar parameters determined by Fuhrmann (1998, 2000), where the effective temperatures are derived from the wings of the Balmer lines; surface gravities are taken from the strong line wings of the Mg Ib triplet and compared with values obtained from Hipparcos parallaxes. Iron abundances are based on Fe II lines, and the microturbulence velocities are estimated by requesting that the iron abundance derived from Fe II lines should not depend on equivalent width. The uncertainties for the temperature, surface gravity, metal abundance and microturbulence velocities are generally assumed to be ± 80 K, 0.1 dex, 0.2 km s^{-1} and 0.07 dex respectively (see Fuhrmann 1998 and 2000 for details). For the Procyon, the parameters were taken from Korn et al. (2003), where the temperatures are again from the wings of Balmer lines; surface gravities are based on the HIPPARCOS parallaxes, and iron abundances are taken from NLTE calculations.

Following Fuhrmann's work, we employ the macroturbulence parameters ζ in the radial-tangential form and adopt values as described in Gray (1984). The projected rotational velocity is obtained as the residual to the observed line profiles, after having removed the known instrumental profile obtained from the Moon spectra.

4. NLTE line formation

4.1. Atomic model

The model of Na we adopt goes back to the atomic properties documented in Baumüller et al. (1998), where most of the problems have been described in detail. In this paper, we extend the number of levels to $n = 15$. The model is closed with the Na$^+$ ground state. Fine structure splitting is neglected with the exception of $3p^2P^0_{1/2}$ and $3p^2P^0_{3/2}$. Part of that model was shown by Baumüller et al. (1998, see their Fig. 2). Energy levels are taken from Martin & Zalubas (1981) if available. For levels with $l \geq 4$ hydrogenic approximations are used. All bound-free radiative cross-sections have been included from close-coupling calculations of Butler (1993) and Butler et al. (1993).

To establish the influence of deviations from LTE on the ionization equilibrium of sodium, we have chosen the reference stars of Korn et al. (2003). The full analysis of the solar spectrum (Kurucz et al. 1984) and those of the reference stars allows a reasonable choice of the hydrogen collision enhancement factor resulting in S$_H = 0.05$ for Na , found by iteration together

Table 1. Atomic data of Na lines. $\log gf$ values and damping constants have been determined from solar spectrum fits

λ [Å]	Transition	$\log gf$	$\log C_6$
5682.642	$3p\,{}^2\mathrm{P}^0_{1/2} - 4d\,{}^2\mathrm{D}_{3/2}$	-0.72	-30.05
5688.214	$3p\,{}^2\mathrm{P}^0_{3/2} - 4d\,{}^2\mathrm{D}_{5/2}$	-0.47	-30.05
5889.959	$3s\,{}^2\mathrm{S}_{1/2} - 3p\,{}^2\mathrm{P}^0_{1/2}$	+0.11	-31.60
5895.932	$3s\,{}^2\mathrm{S}_{1/2} - 3p\,{}^2\mathrm{P}^0_{3/2}$	-0.19	-31.60
6154.228	$3p\,{}^2\mathrm{P}^0_{1/2} - 5s\,{}^2\mathrm{S}_{1/2}$	-1.57	-29.78
6160.751	$3p\,{}^2\mathrm{P}^0_{3/2} - 5s\,{}^2\mathrm{S}_{1/2}$	-1.28	-29.78
8183.260	$3p\,{}^2\mathrm{P}^0_{1/2} - 3d\,{}^2\mathrm{D}_{3/2}$	0.28	-30.73
8194.800	$3p\,{}^2\mathrm{P}^0_{3/2} - 3d\,{}^2\mathrm{D}_{5/2}$	0.49	-30.73

Fig. 1. Comparison of derived [Na/Fe] for stars in common with other studies. Filled circles (●) are from Baumüller et al. (1998); crosses (×) are from Feltzing & Gustafsson (1998); asterisks (∗) are from Carretta et al. (2000); pluses (+) are from Fulbright (2000); diamonds (◇) are from Gratton et al. (2003); opened circles (○) are from Takeda et al. (2003); triangles (△) are from Reddy et al. (2003).

with all basic stellar paraeters. This number is the same as in the previous work of Baumüller et al. (1998).

All calculations have been carried out with a revised version of the DETAIL program (Butler & Giddings 1985) using accelerated lambda iteration (see Gehren et al. 2001, 2004 for details).

4.2. Atomic line data

As our primary choice we take the oscillator strengths from the NIST data base. We note that the gf values are similar to those adopted by Takada et al. (2003), the average difference $\log gf$(this work)$- \log gf$(Takeda) is -0.02 ± 0.04. For the line pair of 6154/6160, our gf values are same as the values adopted by Chen et al. (2000), but slightly higher than the values of Edvardsson et al. (1993) and Feltzing & Gustafsson (1998), the difference is about 0.04. However, in our present analysis the absolute value of the oscillator strengths is unimportant because the abundances are evaluated in a fully differential way with respect to the sun.

Collisional broadening through van der Waals interaction with hydrogen atoms is important for strong Na D lines. As already pointed out by Gehren et al. (2001, 2004) the resulting values of the van der Waals damping constants are mostly near those calculated according to Anstee & O'Mara's (1991, 1995) tables. Fitting the solar profiles with a common Na abundance then shows that our damping constants for the resonance lines are roughly a factor of 2 below those calculated. The adopted line data (gf values and van der Waals damping constants) are given in Table 1.

4.3. Sodium abundances

The abundance determinations for our program stars are made using spectral synthesis. The synthetic spectra are convolved with macroturbulence, rotational and instrumental broadening profiles, in order to match the observed spectral lines. **Based on 5682/5688, 5890/5896 and 6154/6160 line pairs, our abundance results are obtained from profile fits. However, for** Na D lines, as pointed out by Baumüller et al. (1998), even in the solar atmosphere the inner cores of the lines are affected by deviations from LTE. We note that even for some metal-poor stars, only the line wings can be fitted in LTE. So the sodium
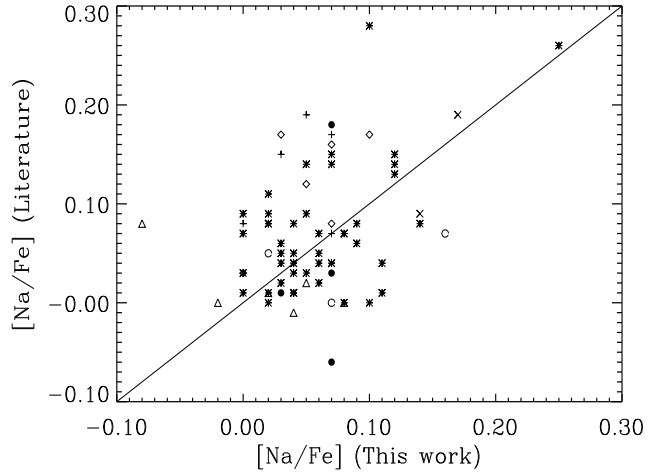
abundances are obtained until a best fit to the observed line wings is provided for the LTE analyses. Considering the NLTE abundances, out results do not show large abundance differences between different lines (however, see Takeda et al. 2003). **The final abundance scatter of single line is between 0.01 and 0.06 with** $< \sigma[\mathrm{Na/Fe}]> = 0.020 \pm 0.007$ **for all stars.** The derived abundances are presented in Table 2. **Complete results for individual lines of all stars can be obtained from the author on request.**

4.4. Comparison with other works

Sodium abundances have been determined by several groups including both LTE and NLTE analyses. In Fig.1 we compare the [Na/Fe] values **(NLTE)** determined in this paper with those from the literature. The agreement is generally good. However, a closer inspection reveals some systematic differences. In the remaining part of this section we will briefly discuss some possible reasons for these differences.

Baumüller et al. (1998)

Baumüller et al. (1998) performed a full NLTE line formation for a sample of metal-poor stars. We have four stars in common with theirs. Our NLTE results are very much in agreement with theirs, as shown in Fig. 1. The average differences between our [Na/Fe] and theirs are 0.02 ± 0.10. We note that the considerable scatter is mostly due to the different stellar parameters adopted.

Feltzing & Gustafsson (1998)

In this study of 47 G and K metal-rich stars, they confirmed the increase of [Na/Fe] as a function of [Fe/H] found previously by Edvardsson et al. (1993). Their results were determined from 6154/6160 lines, the gf values adopted in this study are slightly lower than ours, the differences are $-0.02/-0.05$, re-

spectively. The sodium abundance determined by this study is in a good agreement with ours. For three stars in common, the average difference is 0.01 ± 0.04.

Carretta et al. (2000)

This work reanalysed the data of Edvardsson et al. (1993) including a NLTE correction. They found no large differences from the LTE results of Edvardsson et al., which is shown in their Fig. 9. The gf values of the 6154/6160 lines adopted by Edvardsson et al. (1993) are slightly lower than ours, the differences are -0.04 and -0.03, respectively. The results of Carretta et al. (2000) are very much in agreement with ours. For the 46 common stars from Edvardsson et al. (1993), the average difference between ours and theirs is -0.01 ± 0.05.

Fulbright (2000, 2002)

This analysis deals with a large number of metal-poor stars, of which **five** stars are in common with our sample. As pointed out by Gehren et al. (2004), there are large differences in stellar parameters; on average, the typical difference in temperatures for the individual star is about 150 K, and there are a few stars for which differences may be much larger. Fulbright's abundances are slightly larger than ours (see Fig. 1). For the five stars in common with our list we obtain $\overline{\Delta[\mathrm{Na/Fe}]} = -0.09 \pm 0.05$. We find that the largest difference (~ 0.4 dex) comes from warm metal-poor stars such as HD 284248. We note that considerable discrepancies remain even after correcting for the difference in effective temperatures. As these stars are metal-poor, they may suffer from relatively large NLTE effects (see Sect 5.1).

Gratton et al. (2003)

The authors considered NLTE corrections and reported the sodium abundances for 150 field subdwarfs and subgiants. Our results are mostly in agreement with theirs. For the six stars in common, the average difference is 0.07 ± 0.05.

Takeda et al. (2003)

Very recently, Takeda et al. (2003) performed a NLTE analysis of sodium abundances for disk and halo stars. They reanalysed the data from Chen et al. (2000). Their results vary from line to line (see their Tables 4 and 5). The results for the 6154/6160 lines show no large differences from those of Chen et al. (see their Fig. 5c). Our [Na/Fe] values are in agreement with theirs for the lines of 6154/6160 Å for the three stars in common; the average difference is 0.04 ± 0.06. As already pointed out by Takeda et al., this line pair is not very sensitive to the NLTE effects.

Reddy et al. (2003)

This sample consists of 187 F and G dwarfs. The sodium abundances were based on 6154/6160 lines, the gf values adopted in their work are nearly same as those we adopted. A very close star by star agreement between the [Na/Fe] ratios derived here and those measured by Reddy et al. can be found, no difference exceeds 0.20 dex. For the six stars in common, we obtain $\overline{\Delta[\mathrm{Na/Fe}]} = 0.00 \pm 0.08$. The large scatter is due to HD 218470 (0.16 dex). This is a high $v \sin i$ (13.1 km s^{-1}), high temperature ($T_{\mathrm{eff}} = 6407$) and low gravity ($\log g = 4.02$)

star. For this star their temperature is about 70 K higher than ours.

5. Discussion

5.1. NLTE effects

The abundance analyses of sodium clearly show the NLTE effect. There is a tendency that the NLTE effect is large for warm metal-poor subgiant stars, as would be expected. Baumüller et al. (1998) show in their Fig. 11, that the NLTE line cores for the Na D lines are much deeper than in LTE in metal-deficient stars. In LTE abundance analyses this is compensated by simply increasing the sodium abundance until the observed equivalent width is reproduced. Such results are displayed in Table 3 of Baumüller et al. (see also their Table 2). The results confirm, starting from the solar abundance towards the lower metallicity, that the NLTE abundance effect resulting from the Na D lines increases reaching a maximum near [Fe/H]= -2. LTE abundances can be significantly different from their NLTE counterparts, with differences reaching more than 0.6 dex in extreme cases. In Table 3 it is evident that the NLTE effects are systematically stronger for the hotter models, which is in agreement with the statistical equilibrium of both aluminium and magnesium (Baumüller et al. 1997; Zhao & Gehren 2000). As expected, the strongest departures from LTE are found for models with high temperature and low metallicity. The reduction of surface gravity results in a decreased efficiency of collisions with electrons and hydrogen atoms, which again leads to stronger NLTE effects. In Fig. 2, the differences between LTE and NLTE analyses for our program stars are plotted as a function of metal **abundance, temperature and luminosity**.

It should be noted that the NLTE effects differ from line to line, reflecting their individual properties. For example, the 8183/8194 lines show relatively large NLTE effects compared to the other lines at similar line-strength. From Table 3, we can see the importance of the NLTE effect on different lines in sodium abundance determination:

- the weak 6154/6160 lines show the smallest NLTE abundance effects (≤ 0.1 dex) for the disk stars, so they are the best abundance indicators for LTE analyses of moderately metal-poor stars.
- the NLTE corrections for 5682/5688 lines are relatively small (~ 0.1 dex) for dwarfs; but they increase for subgiants (> 0.1 dex). Therefore these lines should no longer be analyzed with LTE.
- for the 5890/5896 lines, which are important for determining the sodium abundances of very metal-deficient stars, it is necessary to take account of the NLTE effects except for very cool and metal-rich dwarfs. Especially for warm metal-poor giants, the NLTE correction can reach 0.6 dex (see Table 3 for details).
- the 8183/8194 lines are also important for determining the sodium abundances of very metal-deficient stars because of their strength. We suggest that, even for cool metal-rich stars, the NLTE effects should be taken into account.
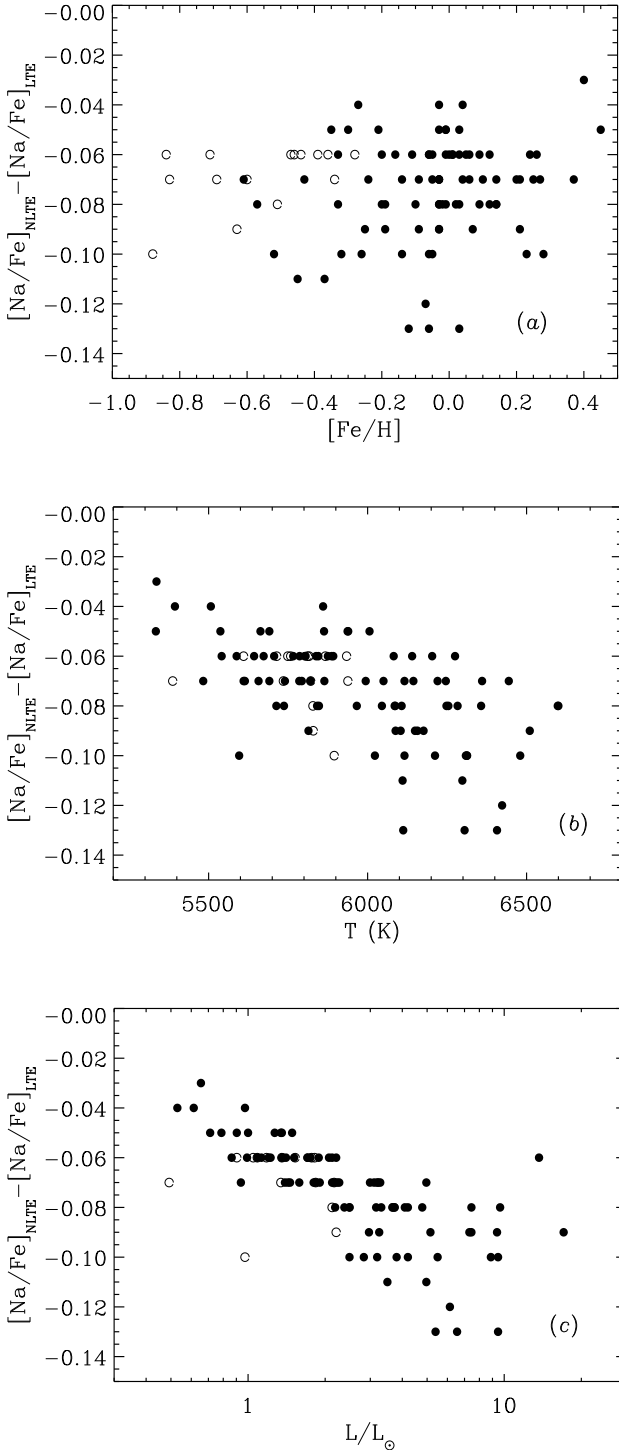
Fig. 3. Abundance ratios [Na/Fe] for NLTE analyses. The meaning of the symbols is the same as in Fig. 2

aimed at. The data may vary considerably whenever the microturbulence velocity deviates from the $1 \, \mathrm{km \, s^{-1}}$, and any simple correction may result in an increased scatter. The reference to [Na/Fe] = 0 may also be a bad approximation, particularly in metal-poor stars.

5.2. Sodium abundance and nucleosynthesis in the Galaxy

The variation of [Na/Fe] with the stellar metal abundance [Fe/H] contains information about the chemical evolution of the Galaxy. Fig. 3 displays the run of [Na/Fe] ratio (calculated in NLTE) with the overall metal abundance for all stars considered in this paper. One important feature that can be seen from Fig. 3 is that the bulk of the sodium abundances **scale approximately as iron** in thin-disk stars, with a small overabundance for the thick-disk stars. The "upturn" in [Na/Fe] versus [Fe/H] for metal-rich disk stars, as observed by Edvardsson et al. (1993), is also reproduced [1].

Using magnesium instead of iron as the reference can remove Type Ia SNe from consideration, because nearly all the sodium and magnesium **are** produced in massive stars (Timmes et al. 1995). Calculations of nucleosynthesis for SNe Ia show that they should produce only very little amounts of sodium (Nomoto et al. 1997). The odd-even effects will be enhanced using magnesium as the basis of comparison. The overall behaviour of [Na/Mg] ratios versus [Mg/H] is therefore shown in Fig. 4 where the Mg abundances are taken from Fuhrmann (1998, 2000). We confirm Arnett's (1971) prediction that [Na/Mg] ratios decline with decreasing metallicity. This suggests that sodium abundances may be more closely coupled to chemical evolution history, with a gradual enrichment of [Na/Mg] from thick to thin disk.

Fig. 2. Difference of [Na/Fe] abundance ratios calculated under NLTE and LTE assumptions as a function of metal abundance (a), temperature (b) and luminosity (c). Filled circles refer to the thin-disk stars, opened circles refer thick-disk stars.

We confirm that departures from LTE of the Na level populations appear to be larger for warm and giant stars, which was also found by Baumüller et al. (1998) and Takeda et al. (2003).

A warning is appropriate that Table 3 should not be used for LTE abundance corrections if precise Na abundances are
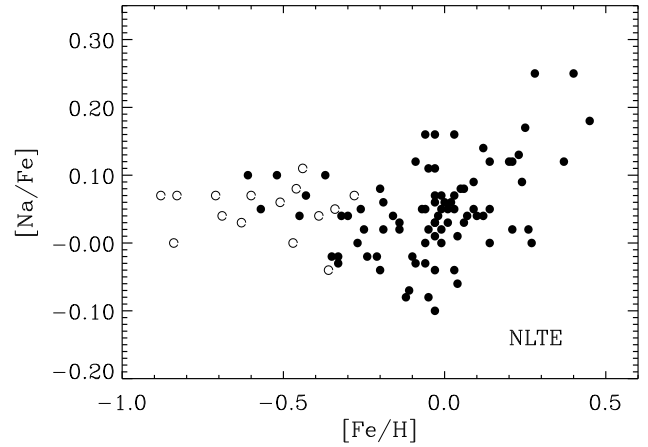
---

[1] We have 47 stars common with the work of Edvardsson et al. (1993). And we note that much more metal-rich stars are included in our sample. The upturn in [Na/Fe] vs. [Fe/H], as observed by Edvardsson et al. is reproduced and reinforced. We confirm that the upturn is real (also see Feltzing & Gustafsson (1998).

Table 3. Abundance differences between NLTE and LTE obtained by fitting calculated LTE *equivalent widths* of Na I lines using the same parameters for various stellar model atmospheres based on the line-blanketed model grid. Results refer to $\Delta[\mathrm{Na/Fe}]= [\mathrm{Na/Fe}]_{\mathrm{NLTE}}- [\mathrm{Na/Fe}]_{\mathrm{LTE}}$. No entries are given for extremely weak lines. The calculations all refer to $\xi = 1$ km s^{-1} and [Na/Fe] $= 0$

| T_{eff}	$\log g$	[Fe/H]	5682	5688	5890	5896	6154	6160	8183	8194	$\overline{\Delta[\mathrm{Na/Fe}]}$
5200	4.50	0.0	-0.08	-0.07	-0.04	-0.04	-0.04	-0.05	-0.15	-0.15	-0.08 ± 0.05
5200	4.50	-1.0	-0.06	-0.06	-0.07	-0.08	-0.04	-0.04	-0.24	-0.24	-0.10 ± 0.07
5200	4.50	-2.0			-0.14	-0.17					-0.15 ± 0.02
5200	4.50	-3.0			-0.17	-0.17					-0.17 ± 0.00
5200	3.50	0.0	-0.14	-0.14	-0.04	-0.06	-0.06	-0.06	-0.31	-0.31	-0.14 ± 0.09
5200	3.50	-1.0			-0.14	-0.16			-0.42	-0.46	-0.29 ± 0.15
5200	3.50	-2.0			-0.31	-0.34					-0.32 ± 0.02
5200	3.50	-3.0			-0.36	-0.28					-0.32 ± 0.04
5780	4.50	0.0	-0.08	-0.08	-0.05	-0.06	-0.04	-0.05	-0.20	-0.21	-0.10 ± 0.05
5780	4.50	-1.0	-0.06	-0.07	-0.16	-0.18	-0.05	-0.05	-0.27	-0.29	-0.14 ± 0.08
5780	4.50	-2.0	-0.05	-0.05	-0.34	-0.32	-0.05	-0.05	-0.10	-0.12	-0.13 ± 0.10
5780	4.50	-3.0			-0.23	-0.16					-0.19 ± 0.04
5780	3.50	0.0	-0.17	-0.18	-0.10	-0.10	-0.06	-0.08	-0.43	-0.43	-0.19 ± 0.12
5780	3.50	-1.0	-0.11	-0.11	-0.33	-0.35			-0.39	-0.43	-0.29 ± 0.12
5780	3.50	-2.0			-0.56	-0.52					-0.54 ± 0.02
5780	3.50	-3.0			-0.27	-0.17					-0.22 ± 0.05
6500	4.50	0.0	-0.07	-0.09	-0.11	-0.15	-0.03	-0.04	-0.28	-0.30	-0.13 ± 0.08
6500	4.50	-1.0			-0.38	-0.41			-0.25	-0.30	-0.33 ± 0.06
6500	4.50	-2.0			-0.45	-0.38					-0.41 ± 0.04
6500	4.50	-3.0			-0.13	-0.10					-0.11 ± 0.02
6500	3.50	0.0	-0.12	-0.13	-0.22	-0.31	-0.05	-0.06	-0.47	-0.52	-0.23 ± 0.15
6500	3.50	-1.0			-0.64	-0.61			-0.32	-0.40	-0.49 ± 0.02
6500	3.50	-2.0			-0.54	-0.43					-0.49 ± 0.06
6500	3.50	-3.0			-0.13	-0.09					-0.11 ± 0.02
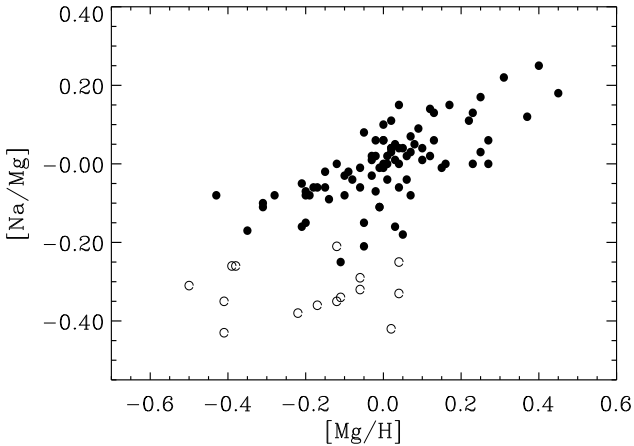
Fig. 4. [Na/Mg] abundances ratios for NLTE analysis as a function of [Mg/H]. Symbols are the same as in Fig. 2

the $Z = 0.02$ for a 20 $M_\odot$ model, while Woosley & Weaver (1995) predict that for a 22 $M_\odot$ SN model, the amount of sodium decreases with increasing metallicity in the range of $Z = 0$ to $Z_\odot$. Also, *AGB stars are potential sites for the production of primary sodium* (Mowlavi 1999). In this scenario synthesis of sodium can occur in hydrogen-burning shells during ON-cycling (Denissenkov & Tout 2000). This process is supported by observations of red giant stars in globular clusters that appear to be sodium-rich (Kraft et al. 1997; Gratton et al. 2001).

Detailed modelling of the Galactic chemical evolution has been attempted by many authors (e.g. Timmes et al. 1995; Goswami & Prantzos 2000). Based on Woosley & Weaver's (1995) metallicity-dependent yields, the first authors calculate the behaviour of [Na/Fe] as a function of metallicity. Their results predict that [Na/Fe] decreases from [Fe/H] ~ -3 to ~ -1.5, while it increases from [Fe/H] ~ -1.5 to ~ -0.5 (see their Fig. 17). However using the same yields with an iron yield reduced by a factor of 2, Goswami & Prantzos' calculation explains the decline of [Na/Fe] from [Fe/H]~ -1 to [Fe/H] ~ -2 reasonably well. And their prediction suggests an everdecreasing [Na/Fe] toward the lower metallicity regime. They used a different initial mass function (IMF), and a different halo model.

Presently, the source of sodium remains to be confirmed. Thus it is difficult to use sodium as a probe of Galactic chemical evolution until the effects of individual stars can be quantified. Theoretical sodium yields of SN II have not yet converged to consistency among models of different authors (Woosley & Weaver 1995; Umeda et al. 2000). Umeda et al. (2000) show the yields of sodium are much less for $Z = 0$ compared to

Our observational results provide some implications for the nucleosynthesis of sodium. We note that in halo stars, sodium

is significantly underabundant relative to iron, and [Na/Fe] (or [Na/Mg]) increases with metallicity (**Fig. 5**). In the region of overlapping metal abundances [Na/Fe] shows a clear distinction between halo and thick-disk stars. The linear relationship indicates that sodium production is connected to the metallicity of the progenitor SN as suggested by Nissen & Schuster (1997). This result agrees with nucleosynthesis calculations of massive stars by Umeda et al. (2000), but it is at variance with the calculations by Woosley & Weaver (1995). We note that there are no extremely metal-poor stars in the sample of Gehren et al. (2004), whereas McWilliam et al. (1995) find that, for stars with [Fe/H] ≤ -3, [Na/Fe] rises with decreasing metal abundance. Based on this result Tsujimoto et al. (2002) argued that sodium yields decrease with increasing Z for the very metal-poor stars. However, nearly all of the stars are giants and the abundances were derived from the Na D (5890/5896) lines, which are very sensitive to NLTE effects (see Sect. 5.1; Takeda et al. 2003). There are two possibilities to explain the high [Na/Fe] values of McWilliam et al.,

– NLTE corrections for Na D lines are large for metal-poor cool giants, so if it is considered, the [Na/Fe] ratios would show an abundance deficiency (however, see Takeda et al. 2003).
– sodium is also produced in metal-poor giant stars (Goriely & Siess 2001), which could explain why the Pb-stars also have a large sodium content (Van Eck et al. 2001).

A definitive confirmation of the latter assumption will require more detailed nucleosynthesis calculations. And it is highly desirable to include the sample of ultra-low metallicity stars for establishing the behaviour of [Na/Fe] in this region, which is important for investigating the history of the early Galaxy as well as for constructing the model of Galactic chemical evolution.

Based on [Eu/Ba] ratios, Mashonkina et al. (2003) suggested that during the active phase of the thick disk formation evolved low mass stars may enrich the interstellar gas. Our observational results show that [Na/Fe] values are about solar, possibly being slightly overabundant in the thick-disk stars, which would confirm the suggestion that AGB stars may contribute some additional sources of sodium. However, metallicity-dependent SN yields of sodium can not be excluded.

While the origin of the "upturn" for the metal-rich stars is still unclear, Feltzing & Gustafsson (1998) argued that metallicity-dependent SN yields may play a role. Though a rather insufficient fraction of stars in the range of supersolar metal abundances prevents us from making any definitive argument, we suggest that quite large amounts of Na may be produced by proton capture on ^{22}Ne nuclei for AGB stars (Denissenkov & Denissenkova 1990).

5.3. Abundance ratios, kinematics, ages and the Galactic stellar populations

It is important to distinguish the individual membership of stars in our sample. We are aware of that such a discussion requires more than the interpretation of abundance ratios alone.
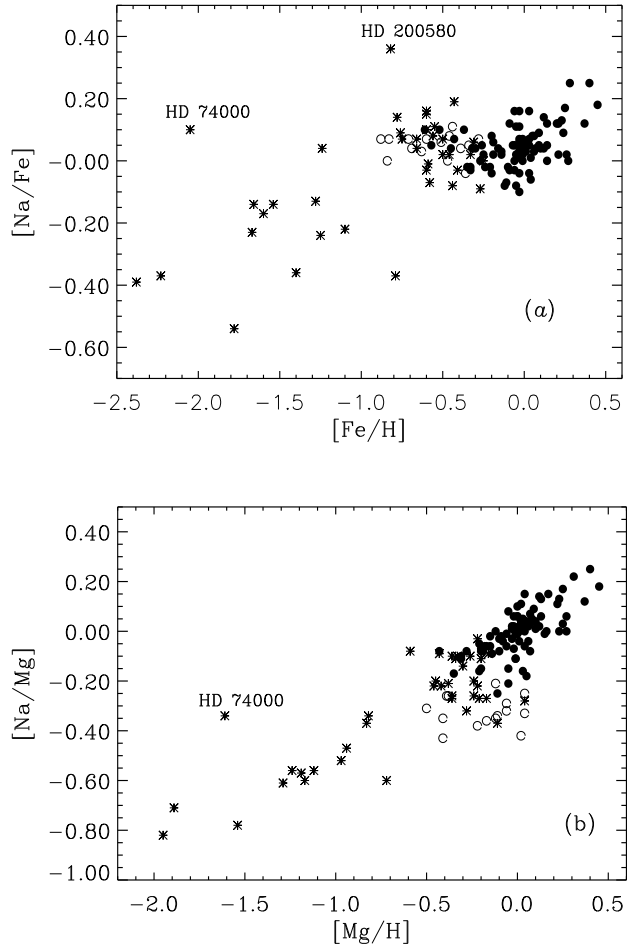

Fig. 5. Top: abundance ratios [Na/Fe] for NLTE analysis as a function of [Fe/H]. Bottom: abundances ratios [Na/Mg] for NLTE analysis as a function of [Mg/H]. Filled and opened circles refer to the thin- and thick-disk stars in this paper, respectively. Asterisks refer to the stars from Gehren et al. 2004

Following Fuhrmann's (1998, 2000) work we use [Mg/Fe] $= 0.25$ as a first step to discriminate between thin- and thick-disk stars.

5.3.1. Abundance ratios and population membership

Fuhrmann (1998) attributed the scatter in [Mg/Fe] to a mixing of thin- with thick-disk stars and a different chemical evolution of these two stellar populations (see also Gratton et al. 2000; 2003 for remarks on O and Mg with respect to Fe). He suggested that the stars with higher [Mg/Fe] at a given [Fe/H] are old thick-disk stars (see also Reddy et al. 2003).

We show the distribution of [Na/Fe] versus [Mg/Fe] for the two populations of thick- and thin-disk stars in Fig. 6. Even comparing abundance alone, Fig. 6 suggests the differences among the two populations: the thin-disk stars are well separated on the left side.
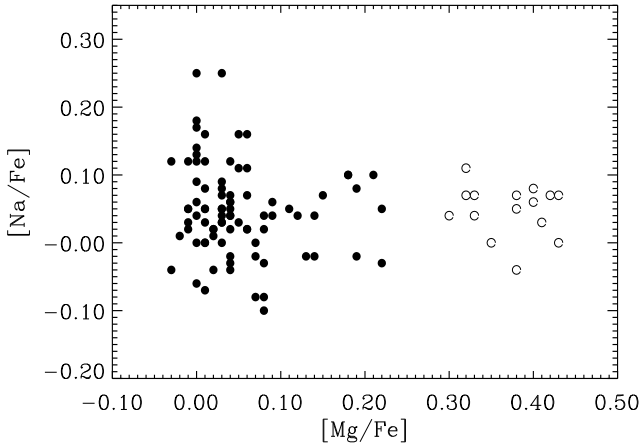
Fig. 6. [Na/Fe] abundances ratios for NLTE analyses as a function of [Mg/Fe]. The meaning of symbols is the same as in Fig. 2

5.3.2. Kinematic properties and population membership

The original classification of stellar populations was based much more on kinematics than on anything else. It is therefore of high priority to check if kinematic properties and abundance ratios have more in common than a coarse change with the mean metal abundance itself. Fuhrmann (2000; 2002; see also Ryan & Smith 2003) argues that in fact halo stars may constitute an extremely small minority of all Galactic stars, whereas most of the stars with intermediate kinematics instead belong to the thick-disk. Fuhrmann (2000) also suggested that there is some kinematical overlap of the disk populations. Therefore the determination of Galactic kinematics provides an important test.

Fuhrmann (2000) has discussed in more detail the kinematical aspects of our sample. The basic data are available in a number of catalogues which are electronically accessible (e.g. via http://www.ari.uni-heidelberg.de/aricns). The correction for the basic solar motion is that of Dehnen & Binney (1998), namely, $U_0/V_0/W_0 = 10.00/5.25/7.17$ km s^{-1}. Whenever these data are not provided, we have calculated the space velocities following the model described by Chen et al. (2000).

The first inspection of the Fig. 7 shows that the V velocities of thin-disk stars tend to be significantly larger than those of the other populations, although there is some overlap between thin- and thick-disk stars. The two most exceptional cases are the thin-disk star HD 52711 (V=−98 km s^{-1}) and the transition star HD 90508 (V=−89 km s^{-1}), and we will come back to them later. The correlation between low [Na/Mg] ratios and low V or high peculiar space velocities (v_{spec}) is also instructive (Fig. 8). The kinematic status in the Toomre diagram of our sample was shown by Fuhrmann (2000 in his Fig. 17).

We now come back to the transition stars HD 90508 ($U/V/W = 31/ − 89/30$ km s^{-1}) and thin-disk object HD 52711 ($U/V/W = −17/ − 98/ − 13$ km s^{-1}): Fuhrmann (2000) argues that although HD 90508 shows thick-disk kinematics, its chemistry and age are more **like** thin-disk stars.
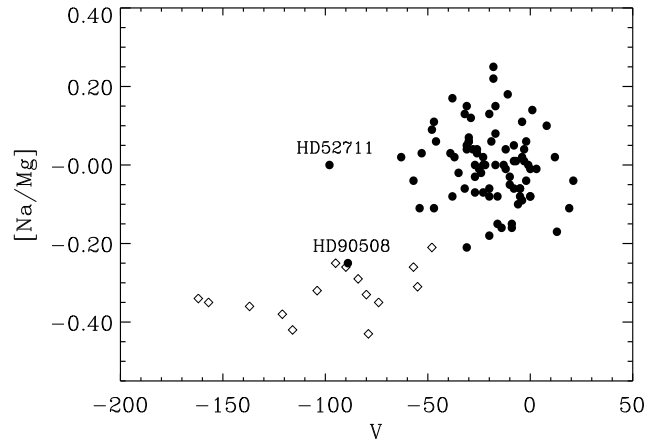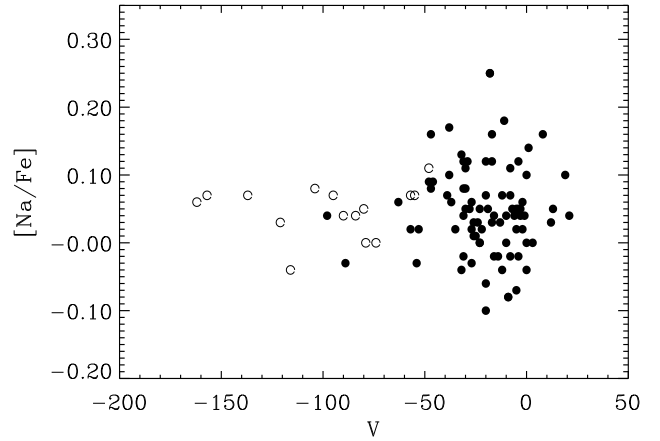

Fig. 7. Correlation between Na abundance ratios and orbital V velocity components. Symbols are as in Fig. 2

HD 52711 is thought to be a thick-disk star based on its *kinematics* (e.g. Ibukiyama & Arimoto 2002), however, it is very young (6.8 Gyr) and [Mg/Fe] is about solar (0.04), therefore it is also more like a thin-disk star.

5.3.3. Stellar ages and population membership

We now turn to the age aspects of analyzed stars. Gratton et al. (2000) concluded that there is a gap in the distribution of [O/Fe] as expected from a sudden decrease in star formation during the transition from the thick- to thin-disk phase. Fuhrmann (2000) suggested that *the key feature to identify thick- and thin-disk stars individually is provided by the stellar ages, while there is a considerable age overlap between halo and thick-disk stars.*

Using the stellar effective temperatures together with the absolute magnitudes based on Hipparcos parallaxes, masses and approximate ages can be interpolated according to [Fe/H] and [α/Fe] from adequate tracks of stellar evolution. Such calculations have recently become available through the work of VandenBerg et al. (2000, 2002) and Yi et al. (2003). In this paper we adopt the Yonsei-Yale isochrones (Yi et al. 2003) since the evolutionary tracks of VandenBerg contain only metal-poor
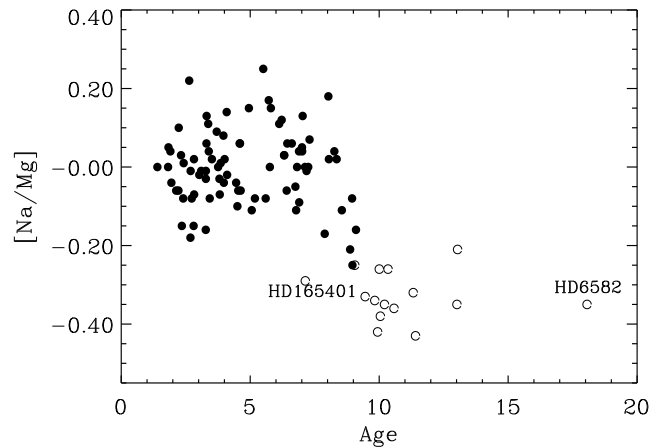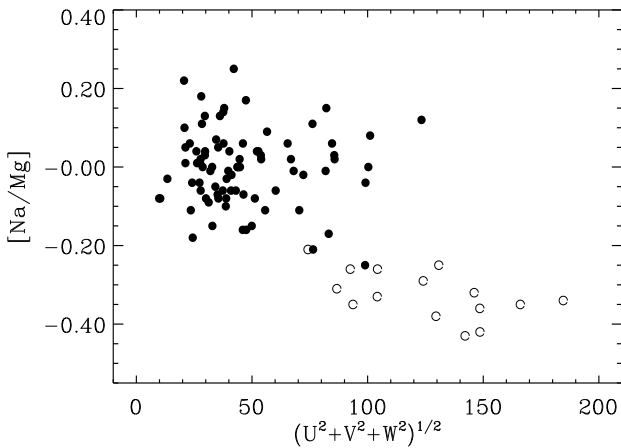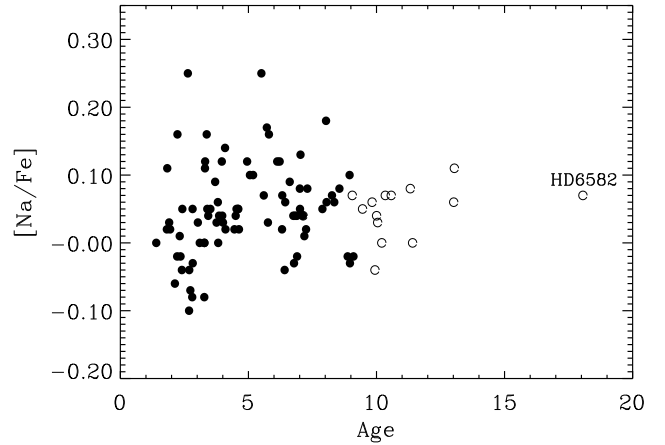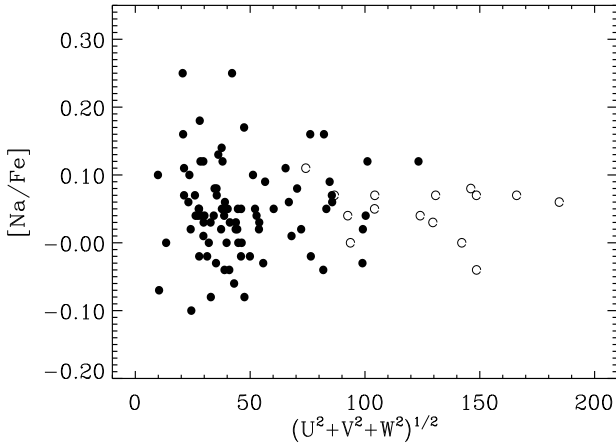
Fig. 8. Correlation between [Na/Fe] abundance ratios and peculiar space velocities $v_{spec} = (U^2 + V^2 + W^2)^{1/2}$ (top), and correlation between [Na/Mg] abundance ratios and peculiar space velocities $v_{spec} = (U^2 + V^2 + W^2)^{1/2}$ (bottom). The meaning of the symbols is the same as in Fig. 2

Fig. 9. Relation of [Na/Fe] ratios vs. stellar ages (top), and relation of [Na/Mg] abundances ratios vs. stellar ages (bottom). Ages are in Gyr. Symbols have the same meaning as in Fig. 2

([Fe/H] $\leq$ −0.31) and low mass stars (M$_{sun}$ $\leq$ 1.20). The Yonsei-Yale isochrones are calculated with new OPAL opacities and Kurucz model atmospheres for a set of metallicities Z = 0.00001, 0.0001, 0.0004, 0.001, 0.004, 0.007, 0.01, 0.02, 0.04, 0.06, 0.08, and [α/Fe] = 0.0, 0.3, 0.6. The mixing length and helium enrichment rate were fixed to $\alpha \equiv l/H_p = 1.7431$ and $\Delta Y/\Delta Z = 2.0$, respectively. The full set of stellar models and a FORTRAN package that works for mass, **metallicity and** α-enhancement interpolation are available from the authors.

The ages derived here are based on the assumption that [O/Mg]= 0. From Fig. 9 we can see that all the thin-disk stars do not exceed $\sim$ 9 Gyr, whereas with the exclusion of HD 165401 all thick-disk stars are older than $\sim$ 9 Gyr. Fuhrmann (1998) identified this star as a thick-disk member with an age of about 10 Gyr, but in his paper II (Fuhrmann 2000) he noted that it is a chromospherically active, high-velocity star, so it was excluded from his later analysis.

As already pointed out by VandenBerg et al. (2002) and iterated by Gehren et al. (2004), a significantly higher [Mg/Fe] ratio could reduce the ages of thick-disk and halo stars by as much as 3 Gyr. For comparison, we also calculated the ages for these stars without α-enhancement. Then our result is fairly in agreement with Fuhrmann's, namely that all the thick-disk (excluding HD 165401) and halo stars are older than 12 Gyr, while all the thin-disk stars are younger than 9.5 Gyr except the three transition stars (HD 90508, HD 143761 and HD 187923). Therefore Fuhrmann's result that *the key feature to identify thick- and thin-disk stars individually is provided by the stellar ages* still holds. However, the 3 Gyr long star formation gap between thin- and thick-disk is not confirmed here.

The three transition stars (HD 90508, HD 143761 and HD 187923) have ages about 8.8 Gyr, thus they are as old as the oldest thin-disk stars. They would be about 10.5 Gyr old if no α-enhancement were considered.

We also note that the age of the thick-disk star HD 6582 seems to be very high (>15 Gyr); Gehren et al. (2004) have discussed this in detail.

6. Conclusions

We have determined sodium abundances for some 90 nearby stars, spanning the range -0.9 < [Fe/H] < +0.4. All abundances are derived from NLTE statistical equilibrium calculations. Based on our results we come to the following conclusions:

1. The [Na/Fe] ratios are about solar for thin- and thick-disk stars. The "upturn" of [Na/Fe] for metal-rich stars is reproduced.
2. The NLTE effects are different from line to line. The 6154/6160 lines are comparatively less sensitive to NLTE effects, while the Na D and near-IR line pairs show large NLTE effects. Large departures from LTE appear for warm metal-poor subgiant stars.
3. Our results suggest that the sodium yields increase with the metallicity, and quite large amounts of sodium may be produced by AGB stars.
4. Combined with the abundance ratios, kinematics and stellar ages, we identify individual thick- and thin-disk stars. Fuhrmann's suggestion that stellar ages provide a key feature in discriminating the two disk populations is supported.

It would be important to perform NLTE abundance determinations for both Mg and Al for these program stars to confirm our identification, because both Al and Mg show large NLTE effects for metal-poor stars (Gehren et al. 2004). And it will be also necessary to investigate some extremely metal-poor stars.

References

Anstee S.D., O'Mara B.J., 1991, MNRAS 253, 549
Anstee S.D., O'Mara B.J., 1995, MNRAS 276, 859
Arnett W.D., 1971, ApJ 166, 153
Baumüller D., Butler K., Gehren T., 1998, A&A 338, 637
Baumüller D., Gehren T., 1997, A&A 325, 1088
Butler K., 1993, unpublished
Butler K., Giddings J. Newsletter on the analysis os astronomical spectra No. 9, University of London
Butler K., Mendoza C., Zeippen C.J., 1993, J. Phys. B 26, 4409
Carretta E., Gratton R.G., Sneden C., 2000, A&A 356, 238
Chen Y.Q., Nissen P.E., Zhao G. et al. 2000, A&AS 141, 491
Dehnen W., Binney J.J., 1998, MNRAS 298, 387
Denissenkov P.A., Denissenkova S.N., 1990, SVAL 16, 275
Denissenkov P.A., Tout C.A., 2000, MNRAS 316, 395
Edvardsson B., Andersen J., Gustafsson B., et al. 1993, A&A 275, 101
Feltzing S., Gustafsson B., 1998, A&AS 129, 237
Fuhrmann K., 1998, A&A 338, 161
Fuhrmann K., 2000, http://www.xray.mpe.mpg.de/~fuhrmann
Fuhrmann K., Axer M., Gehren T. 1993, A&A 271, 451
Fuhrmann K., 2002, New Astr. 7, 161

Fuhrmann K., 2004, AN 325, 3
Fuhrmann K., Pfeiffer M., Frank C. et al. 1997, A&A 323, 909
Fulbright J.P., 2000, AJ 120, 1841
Fulbright J.P., 2002, AJ 123, 404
Gehren T., Butler K., Mashonkina L. et al. 2001, A&A 366, 981
Gehren T., Liang Y.C., Shi J.R. et al. 2004, A&A 413, 1045
Gilmore G., 1995, In van der Kruit, P. C. and Gilmore, G. (eds) IAU Symp. 164, Stellar Populations, Kluwer, Dordrecht, p. 99
Goriely S., Siess L., 2001, A&A 378, L25
Goswami A., Prantzos N., 2000, A&A 359, 191
Gray D.F., 1984, ApJ 281, 719
Gratton R.G., Bonifacio P., Bragaglia A. et al. 2001, A&A 369, 87
Gratton R.G., Carretta E., Castelli F., 1996, A&A 314, 191
Gratton R.G., Carretta E., Claudi R. et al. 2003, A&A 404, 187
Gratton R.G., Carretta E., Matteucci F. et al. 2000, A&A 358, 671
Ibukiyama A., Arimoto N., 2002, A&A 394, 927
Korn A., Shi J.R., Gehren T., 2003, A&A 407, 691
Kraft R.P., Sneden C., Smith G.H., et al. 1997, AJ 113, 279
Kurucz R. L., Furenlid I., Brault J. et al. 1984, Solar Flux Atlas from 296 to 1300nm. Nat. Solar Obs., Sunspot, New Mexico
Limongi M., Straniero O., Chieffi A., 1998, in Stellar Evolution, Stellar Explosions and Galactic Evolution, ed. A. Mezzacappa, London, Inst. Phys., p. 385
Martin W.C., Zalubas R., 1981, J. Phys. Chem. Rev. Data, 153
Mashonkina L., Gehren T., Travaglio C., et al. 2003, A&A 397, 275
McWilliam A., Preston G.W., Sneden C., et al. 1995, AJ 109, 2736
Mowlavi N., 1999, A&A 350, 73
Nissen P.E., Schuster W.J. 1997, A&A 326, 751
Nomoto K., Iwamoto K., Nakasato N. et al. 1997, Nucl. Phys. A621, 467c
Pfeiffer M.J., Frank C., Baumüller D. et al. 1998, A&AS 130, 381
Pilachowski C.A., Sneden C., Kraft R.P., 1996, AJ 111, 1689
Prochaska J.X., Naumov S.O., Carney B.W. et al. 2000, AJ 120, 2513
Reddy B.E., Tomkin J., Lambert D.L. et al. 2003, MNRAS 340, 304
Ryan S.G., Smith I.M., 2003, MNRAS 341, 199
Stephens A., 1999, AJ 117, 1771
Takeda Y., Zhao G., Takeda-Hidai M. et al. 2003, CJA&A 3, 316
Timmes F.X., Woosley S.E., Weaver T.A., 1995, ApJS 98, 617
Tsujimoto T., Nomoto K., Yoshii Y., et al. 1995, MNRAS 277, 945
Tsujimoto T., Shigayama T., Yoshii Y., 2002, ApJ 565, 1011
Umeda H., Nomoto K., Nakamura T., 2000, in The first Stars, eds. A. Weiss, T. Abel & V. Hill, Heidelberg, Springer, p. 150
VandenBerg D.A., Swenson F.J., Rogers F.J. et al. 2000, ApJ 532, 430
VandenBerg D.A., Richard O., Michaud G. et al. 2002, ApJ 571, 487
Van Eck S., Goriely S., Jorisse A. et al. 2001, Nature 412, 793
Woosley S.E., Weaver T.A., 1995, ApJS 101, 181
Yi S. K., Kim Y. C., Demarque P., 2003, ApJS 144, 259
Zhao G., Gehren T., 2000, A&A 362, 1077

Table 2. Atmospheric parameters and sodium abundances of the program stars. Rotational velocities and macroturbulence data are the same as in Fuhrmann (1998, 2000)

HD	T_{eff}	$\log g$	[Fe/H]	ξ	[Na/Fe] LTE	[Na/Fe] NLTE
400	6149	4.06	-0.25	1.31	0.11	0.03
3079	6050	4.17	-0.14	1.42	0.09	0.02
4614	5939	4.33	-0.30	1.06	0.09	0.04
5015	6045	3.90	-0.02	1.39	0.12	0.04
6582	5387	4.45	-0.83	0.89	0.14	0.07
6920	5838	3.48	-0.05	1.35	0.08	0.02
9407	5663	4.42	0.03	0.87	0.09	0.05
9826	6107	4.01	0.09	1.40	0.13	0.04
10697	5614	3.96	0.10	1.04	0.11	0.04
16141	5737	3.92	0.02	1.24	0.14	0.06
16895	6248	4.20	-0.01	1.42	0.08	0.00
18757	5714	4.34	-0.28	0.95	0.13	0.06
18803	5657	4.39	0.14	0.87	0.12	0.05
19373	5966	4.15	0.03	1.23	0.24	0.16
19994	6087	3.97	0.14	1.19	0.20	0.12
20619	5706	4.48	-0.20	0.90	0.02	-0.04
22879	5867	4.26	-0.84	1.21	0.06	0.00
25457	6246	4.32	0.06	1.25	0.10	0.03
30649	5816	4.28	-0.47	1.18	0.06	0.00
30743	6298	4.03	-0.45	1.64	0.15	0.04
34411	5875	4.18	0.03	1.08	0.13	0.07
37124	5610	4.44	-0.44	0.89	0.17	0.11
43042	6444	4.23	0.04	1.52	0.01	-0.06
43386	6480	4.27	-0.06	1.56	0.26	0.16
52711	5887	4.31	-0.16	1.04	0.10	0.04
58855	6309	4.16	-0.32	1.38	0.14	0.04
61421	6600	3.96	-0.03	1.83	0.19	0.11
62301	5938	4.06	-0.69	1.28	0.11	0.04
67228	5847	3.93	0.12	1.18	0.22	0.14
69611	5821	4.18	-0.60	1.22	0.14	0.07
75732	5336	4.47	0.40	0.76	0.28	0.25
90508	5802	4.35	-0.33	1.02	0.03	-0.02
95128	5892	4.27	0.00	1.01	0.12	0.06
102158	5758	4.24	-0.46	1.13	0.14	0.08
102870	6085	4.04	0.14	1.38	0.08	0.00
109358	5863	4.36	-0.21	1.12	0.03	-0.02
114710	6006	4.30	-0.03	1.12	0.08	0.03
114762	5934	4.11	-0.71	1.14	0.13	0.07
117176	5483	3.82	-0.09	1.02	0.04	-0.03
120136	6360	4.17	0.27	1.56	0.07	0.00
121370	6023	3.76	0.28	1.40	0.35	0.25
121560	6144	4.27	-0.43	1.26	0.14	0.07
122742	5537	4.43	-0.01	0.78	0.12	0.07
124850	6112	3.78	-0.06	1.48	0.10	-0.03
126053	5691	4.45	-0.35	0.96	0.03	-0.02
127334	5691	4.22	0.21	0.97	0.18	0.12
130322	5394	4.55	0.04	0.79	0.05	0.01
130819	6598	4.18	-0.10	1.76	0.06	-0.02

Table 2 (continued)

HD	T_{eff}	$\log g$	[Fe/H]	ξ	[Na/Fe] LTE	[Na/Fe] NLTE
132254	6220	4.15	-0.03	1.46	0.10	0.03
134987	5740	4.25	0.25	1.02	0.24	0.17
136064	6116	3.86	-0.05	1.41	0.18	0.11
136202	6104	3.80	-0.09	1.45	0.21	0.12
137052	6283	3.94	-0.03	1.89	-0.02	-0.09
141004	5864	4.09	-0.03	1.05	0.08	0.01
142373	5841	3.84	-0.57	1.24	0.13	0.05
142860	6254	4.02	-0.19	1.36	0.10	0.02
143761	5821	4.12	-0.24	1.10	0.05	-0.02
145675	5334	4.51	0.45	0.81	0.23	0.18
146233	5786	4.36	0.01	0.98	0.09	0.03
150680	5814	3.72	-0.03	1.38	0.25	0.16
153597	6275	4.36	-0.11	1.48	-0.01	-0.07
154345	5507	4.57	-0.03	0.70	0.00	-0.04
157214	5735	4.24	-0.34	1.00	0.12	0.06
157347	5643	4.31	-0.01	0.90	0.08	0.02
159222	5845	4.28	0.09	1.05	0.15	0.09
161797	5596	3.93	0.23	1.17	0.23	0.16
162003	6423	4.06	-0.07	1.67	0.17	0.05
162004	6203	4.24	-0.06	1.29	0.11	0.04
163989	6116	3.62	-0.14	1.61	0.13	0.03
165401	5811	4.41	-0.39	1.10	0.10	0.04
165908	5994	4.01	-0.61	1.25	0.17	0.09
168009	5785	4.23	-0.03	1.03	0.13	0.06
168151	6357	4.02	-0.33	1.68	0.05	-0.02
173667	6305	3.99	0.03	1.60	0.09	-0.04
176377	5860	4.43	-0.27	0.91	0.04	0.00
178428	5673	4.23	0.12	0.96	0.10	0.04
182572	5610	4.19	0.37	1.01	0.19	0.12
184499	5828	4.13	-0.51	1.17	0.14	0.05
186408	5805	4.26	0.06	1.03	0.14	0.08
186427	5766	4.29	0.05	0.89	0.14	0.08
187013	6312	4.09	-0.05	1.46	0.02	-0.08
187691	6088	4.07	0.07	1.35	0.13	0.04
187923	5713	3.97	-0.20	1.19	0.16	0.08
190360	5588	4.27	0.24	0.98	0.15	0.09
190406	5937	4.35	-0.01	1.10	0.10	0.05
204155	5829	4.12	-0.63	1.18	0.12	0.03
207978	6313	3.94	-0.52	1.57	0.20	0.10
209458	6082	4.33	-0.06	1.15	0.05	0.00
210277	5541	4.42	0.26	0.73	0.07	0.02
210855	6176	3.81	0.21	1.61	0.11	0.02
215648	6110	3.85	-0.37	1.69	0.21	0.10
216385	6212	3.85	-0.26	1.54	0.15	0.05
217014	5793	4.33	0.20	0.95	0.19	0.12
218470	6407	4.07	-0.12	1.85	0.05	-0.08
219623	6140	4.23	0.01	1.30	0.11	0.05
221830	5749	4.19	-0.36	1.14	0.02	-0.04
222368	6157	3.95	-0.19	1.51	0.15	0.06
G78-1	5895	4.11	-0.88	1.14	0.17	0.07